

## **Influence of the needle lift motion on cavitating flow inside Diesel injector**

R. Marcer<sup>\*</sup>, C. Audiffren, B. Yerly  
Principia, Zone Athélia 1 – 13705 La Ciotat FRANCE

### **Abstract**

The paper deals with CFD simulations of cavitating flow in a Diesel off center one-hole nozzle. As the hole has an eccentricity with respect to the nozzle symmetry axis, we want first to check the ability of the model to simulate the unsymmetrical cavitation which develops within the hole. For that purpose numerical results are successfully compared with measurements. Then a specific study is dedicated to the assessment of the needle lift motion influence on the cavitation development in the hole and on the flow rate evolution. Comparisons are issued between a full “unsteady” approach where the variable needle lift is considered in the calculation, and a “steady” needle lift approach for which a computation is done with a fixed needle lift. Results show that the steady approach is inaccurate for low lift when the dynamic motion of the needle may have a significant influence on the cavitation development in the hole and so, on the flow rate. However at high needle lift, the steady method gives the same results as the unsteady approach allowing CPU time saving.

---

### **Introduction**

In Diesel injection the flow in the injector, and especially the cavitation development and its influence on the flow rate, is led by the needle lift according to an opening/closing motion cycle. The simulation of that kind of unsteady cavitating flow can be simulated with a CFD model considering a time-varying needle lift. However in this unsteady approach computational time may be large because of the small time steps that are required to represent the cavitation dynamics in the nozzle, especially if a complete needle lift cycle is considered. An interesting possible alternative may be the steady needle lift approach, meaning that the lift is considered as fixed for a given calculation. This approach helps to reduce the simulation time because it allows providing at convergence all the features of flow (including flow rate) for the considered lift, without having to simulate the previous transient opening phase of the lift motion (up to the considered lift). The question is whether the steady approach allows to reproduce the same results as unsteady approach, i.e. for a given needle lift, if simulated flow (flow rate, cavitation) is the same for the steady and unsteady approaches considering that the last one takes into account the dynamic aspects related to the lift motion.

Cavitation simulation in injectors has been the topic of many numerical studies. Various methods can be found in the literature for calculating unsteady cavitation with URANS codes, for example mixture or single-fluid model using a barotropic equation artificially smoothed [1], or based on the Rayleigh-Plesset equation [2], two-fluid formulation of the conservation laws with use of the Rayleigh-Plesset equation for the calculation of the interphase transfer source terms [3], interface tracking method [4].

Due to the experimental evidence that cavitation appears as sheets for real size geometries, at least at the entrance of nozzle holes, the EOLE CFD code developed by Principia uses an improved VOF interface tracking model allowing to compute the unsteady liquid/vapour interface dynamics including mass transfer process at the liquid/vapour interfaces. This code has been widely validated for cavitating flow simulations (see for example in [4], [5], [6]). It will be briefly reminded in the following.

In this study a one nozzle injector with an eccentricity of the hole is concerned. Numerical simulations are performed with both unsteady and steady approaches for the needle lift modeling. Validations of the numerical model based on comparisons with measurements of cavitation carried out at the LMFA [7], are presented.

### **CFD model**

The numerical simulation of two-phase flows with phases separated by sharp interfaces, such as sheet cavitation (as opposed to cavitation bubble flows), requires the simultaneous solution of the Navier-Stokes equations in the two fluids and of the displacement of the interfaces. Among the different kinds of interface tracking methods, the VOF model is one of the most efficient because of its ability to represent complex deformations of interfaces including break-up. Moreover this method can easily be handling to introduce liquid/vapour mass transfer occurring during cavitation process.

---

<sup>\*</sup> richard.marcer@principia.fr

The VOF method introduces a discrete function  $C$  whose value between 0 and 1 in each cell is the fraction of the cell occupied by the liquid. The fraction  $1-C$  of the cell volume is then occupied by vapour (cavitation). The transport of the  $C$  fraction, i.e the motion of the interface in the fixed mesh, is ensured by an eulerian method where a conservation equation of the function  $C$  is solved.

In the code EOLE, the Kinematics and Mass Transfer VOF (KMT-VOF) [6] model is used to simulate both the kinematic motion of the liquid-vapour interface and the thermodynamical mass-transfer process from an added source term in the VOF conservation equation. The mass transfer is taken into account through a semi-empirical cavitation criterion. At each time step, an instantaneous mass transfer is imposed into liquid cells of the mesh having a pressure lower than the vapour pressure, or on the opposite imposed for condensing vapour cells of the mesh having a pressure higher than the cavitation pressure.

So in the KMT-VOF model the position of the liquid-vapour interface computed by the VOF method and representative of the purely kinematic part of the cavitating flow, is then corrected in order to take into account thermodynamical effects. Thus the “kinematic” VOF field is modified in such a way that the interface is constrained to fit the vapour pressure isobar and therefore the pressure of the liquid phase remains higher than the vapour pressure and on the opposite the pressure of the vapour remains close to the vapour pressure. In this model the mass transfer source term is a function of the pressure gradient field.

The liquid phase may be compressible due to the high velocity and pressure gradients existing in the nozzle cavitating flow. The density variation being related to dynamic but not to thermal effect, an equation of state is introduced, where the local density is a function of the local pressure. The molecular viscosity depends also on the pressure, considering isothermal flow conditions. The turbulent nature of the flow is taken into account through a  $k-\varepsilon$  model even if it must be pointed out that turbulence is not a preponderant phenomenon for injection flows. Reynolds numbers remain small, lesser than 20000 in the hole, and strong geometrical constraints limit the development of vortices.

## Model of the injector

The main geometrical characteristics of the studied nozzle with an eccentricity of the hole are the following: length=1mm, diameter=200 $\mu\text{m}$ , radius of curvature of the hole=20 $\mu\text{m}$ , off center of the hole=35 $\mu\text{m}$  (figure 1). The multi-block structured mesh includes 180000 cells for only half of the geometry because of symmetrical conditions. The dynamic motion of the needle in the injector is computed with a grid deformation technique [5] which permits to manage very small needle lift, about 1 $\mu\text{m}$  between the needle and the injector wall (figure 2). The algorithm allows computing a new mesh at each time step, according to the needle lift law. This intermediate mesh is interpolated between two opposite meshes corresponding respectively to the fully closed and fully open positions of the needle, both having the same topology. The hole is discretized from a multi-block O topology which gives more homogeneous cells than H topology for a cylindrical geometry.

Injection pressure ( $P_{inj}=250$  bar) and back pressure ( $P_b=1$  bar) are given as boundary conditions. It can be expected intense cavitation development according to the high value of the corresponding cavitation number  $\sigma=(P_{inj}-P_b)/P_b=249$ .

Density and viscosity of the normafluid are considered. They depend on the pressure.

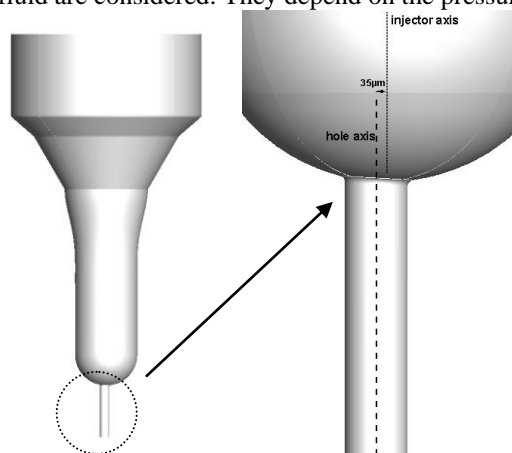


Figure 1: model of the injector with an off center hole

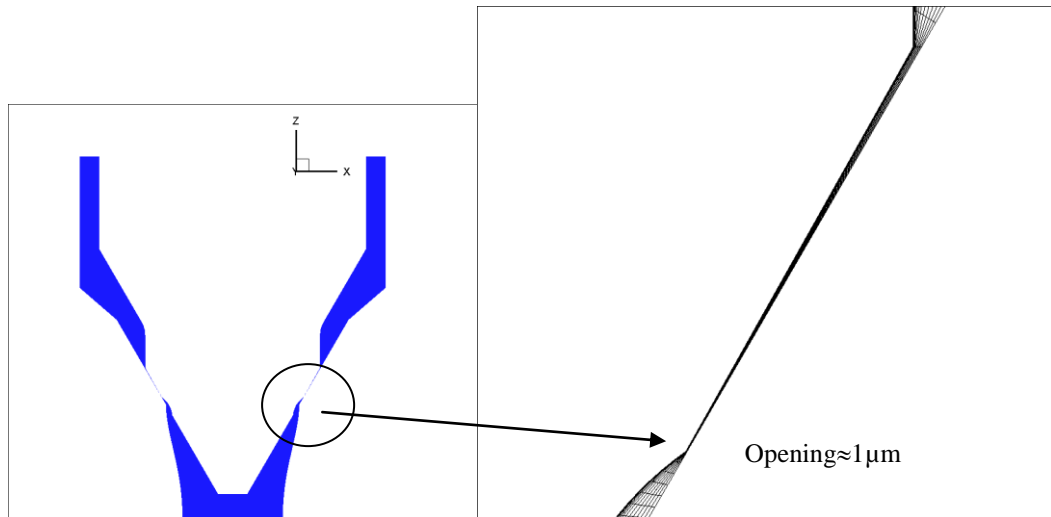


Figure 2: zoom of the mesh in the needle seat at very low lift of the needle

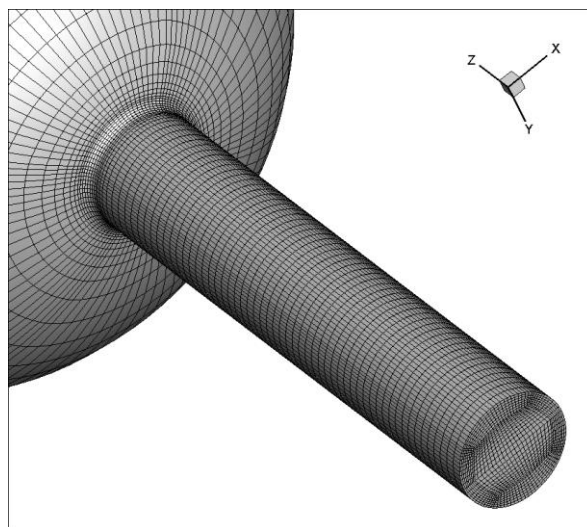


Figure 3: O-topology of the mesh in the hole

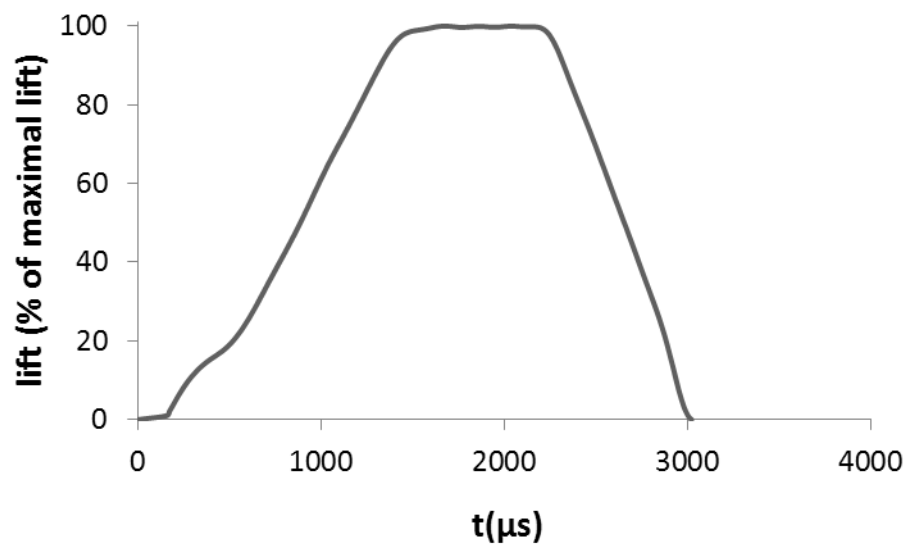
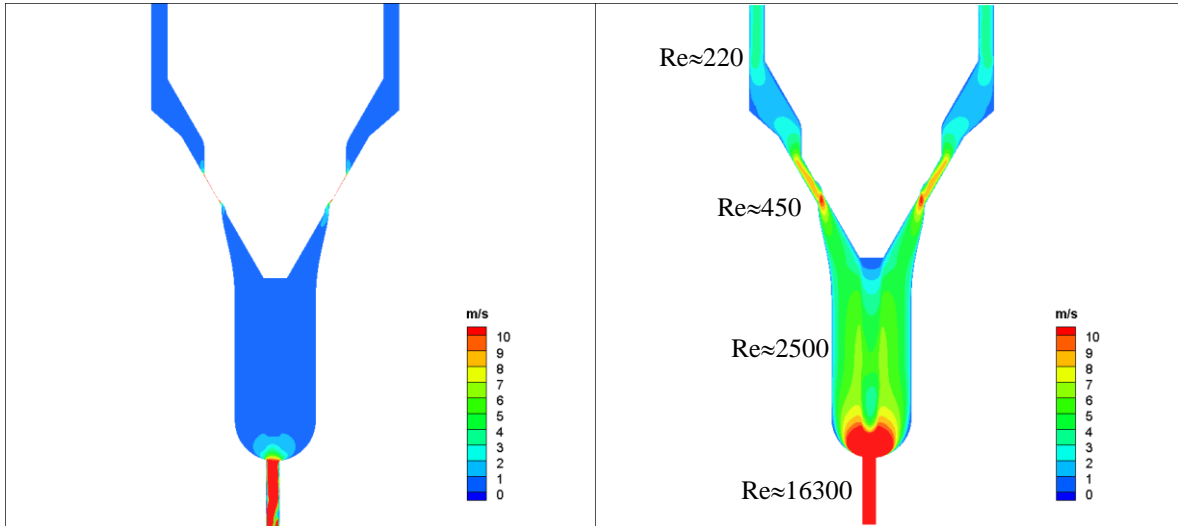


Figure 4: needle lift law

**Results and comparisons with experiments**

First calculations are performed with the time-varying needle lift approach considering the needle lift profile given on figure 4 (with a maximal opening = 270µm).



**Figure 5: velocity at very low needle lift (left) and high lift (right)**

Figure 5 shows the velocity field in the injector at low and high needle lift. Corresponding local Reynolds numbers are mentioned as well. They are built with the local section and the maximal velocity on this section. Except in the hole, the flow velocity remains small whatever the needle lift with maximum values, lesser than 20m/s, in the narrow part of the needle seat. In the hole due to the contraction of the liquid section by the cavitation, the liquid velocity slightly exceeds the theoretical Bernoulli velocity (250m/s against 245m/s) computed from the pressure gradient  $P_{inj}-P_b$ . According to the very small dimensions of the injector, Reynolds number stay small even at high needle lift and the flow remains even laminar except in the hole.

A brief development of cavitation is visible in the needle seat at low lift for which strong geometrical constraints induce a local loss of pressure responsible of the cavitation onset (figure 6). This local cavitation is going to quickly disappear with the needle opening and the associated rising liquid pressure.

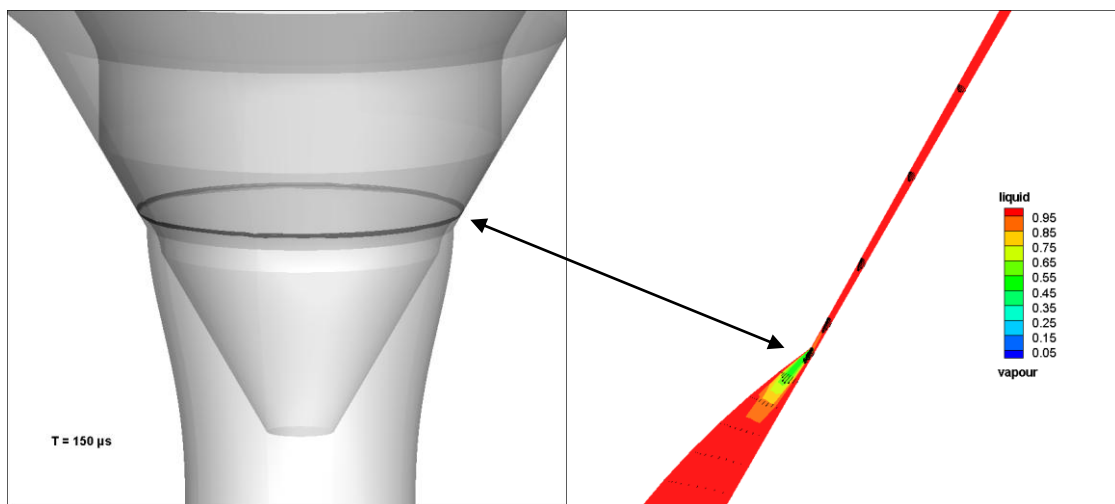


**Figure 6: cavitation in the needle seat at low lift**

Figure 7 shows examples of comparisons of the cavitation pattern issued from experiments and from the computations, at low and high needle lift. In both cases, the onset of cavitation in the hole occurs at low lift (<10% of the maximal lift) and then develops very quickly as the needle is opening up to approximately 15% of the full lift for which a fully developed cavitation is already observed with an extension of the vapour (which appears in black) all along the hole in a dissymmetrical way due to the eccentricity of the hole. For higher lift the cavitation remains unchanged.

Figure 8 shows a snapshot of the cavitation pattern at high lift on a 2D longitudinal section (symmetry plane of the injector). Eccentricity of the hole towards the left with respect to the injector symmetry axis leads the cavitation to mainly develop along the wall on the opposite side of the eccentricity. Indeed the flow separation at the hole inlet which is responsible of the pressure drop and so the onset of cavitation, is more intense on this side (right side on figure 8).

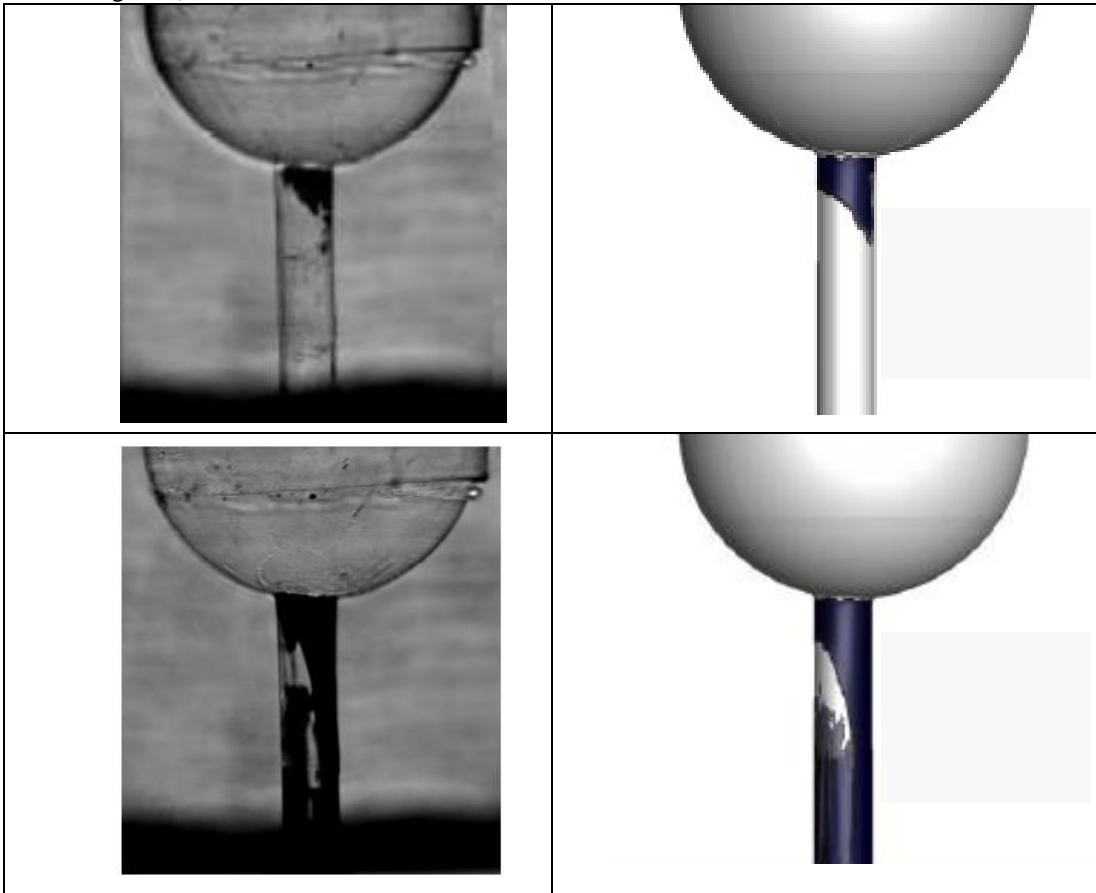


Figure 7: comparison LMFA measurements (left) and CFD (right) of the cavitation (in black) in the hole at low lift (top figures) and at high needle lift (bottom figures)

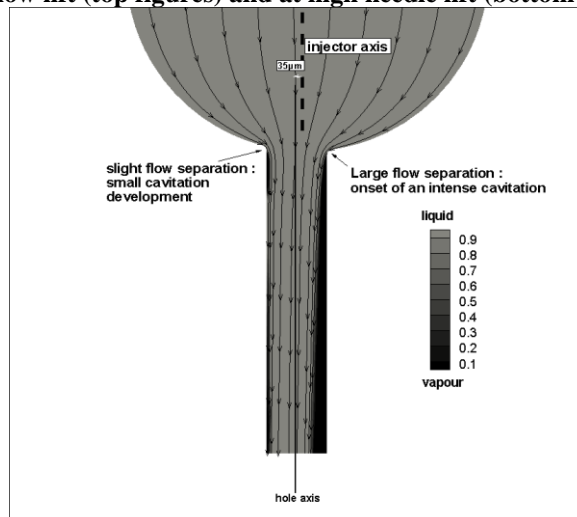
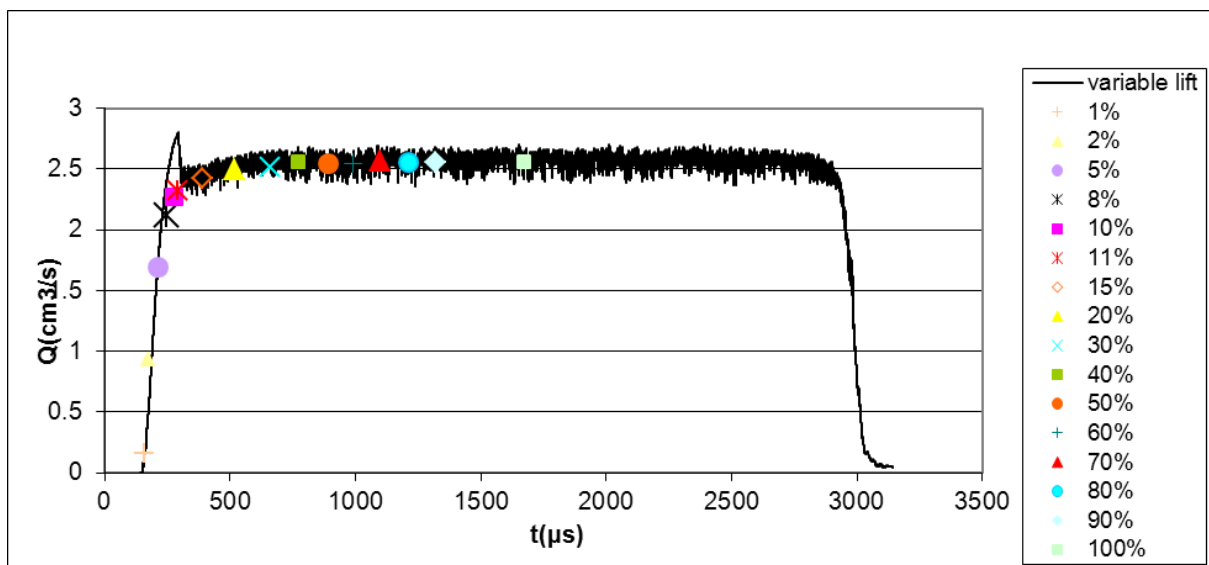


Figure 8: view of the cavitation shape in a plan

### Comparison unsteady/steady approaches for needle lift

The cavitation pattern and the flow rate issued from the time-varying needle lift computation (unsteady approach) considering the needle lift profile given on figure 4 are compared with the steady approach for which the needle is imposed as fixed for each calculation. Note that no experiment data were available for flow rate comparison.

Above 15% of the maximal lift the steady approach gives very similar results according to the unsteady approach, for the flow rate (figure 9) as well as for the cavitation pattern which is fully developed in both cases (see figure 10 and lift  $\geq 15\%$ ). Indeed, the flow rate reaches a quasi-stable value as the cavitation remains steady in the hole for needle opening higher than 15% ( $Q_{20\%} = 97\%$  of the maximal flow rate obtained at full opening of the needle). So, for lift  $\geq 15\%$  the motion of the needle has no influence on the flow.



**Figure 9: flow rate versus needle lift issued from both methods, unsteady (black line) and steady (spotted by symbols in % of maximal lift)**

However at lower needle lift ( $< 15\%$  of the maximal lift) cavitation and flow rate obtained with both approaches are significantly different (figure 10). For the steady approach the flow rate evolves continuously according to the needle lift and the cavitation reaches a fully developed steady state at 8% lift. On the contrary the unsteady approach shows higher flow rate in the range of 8% and 15% lift (figure 10) due on one hand to a cavitation delay compared to the steady approach, and linked on the other hand with a dynamic pulse of cavitation in the hole, responsible of a peak of liquid velocity in the contracted section. Thus the flow rate in this range of low lift exceeds the flow rate reached at high lift (figure 9). Of course this rapid transient dynamic is not highlighted by the steady approach for which the dynamic effect of the needle motion and the associated transient cavitation development is not considered. This transient effect vanishes beyond 15% lift where both steady and unsteady methods show very similar fully developed cavitation shape and flow rate.

For very small lift ( $< 5\%$  of the maximal lift) the steady approach tends to overpredict the flow rate. Indeed in the unsteady method the pressure level in the nozzle progressively raises as the needle is opening whereas for a fixed needle the flow is instantaneously released with a maximal pressure jump between the upstream part of the needle seat (approximately the injection pressure) and the downstream back pressure, leading to an asymptotic value of the flow rate. This overestimation of the flow rate is then directly linked to the inability of the steady approach to account for dynamics effects, especially the pressure behaviour, related to the needle motion which is important at small lift.

Errors up to 20% on flow rate values are thus given by steady approach at low lift which turns out to be inaccurate in this range of needle lift.

It must be pointed out that for 5% lift the two approaches give same flow rate whereas the flow are different, non cavitating for the unsteady approach for which the cavitation appears only at about 8% lift, and cavitating

for the steady approach as early as 2% lift. It appears that the overestimation of the pressure gradient and the flow rate in the steady case is counterbalanced by the presence of the cavitation which tends to limit the flow rate.

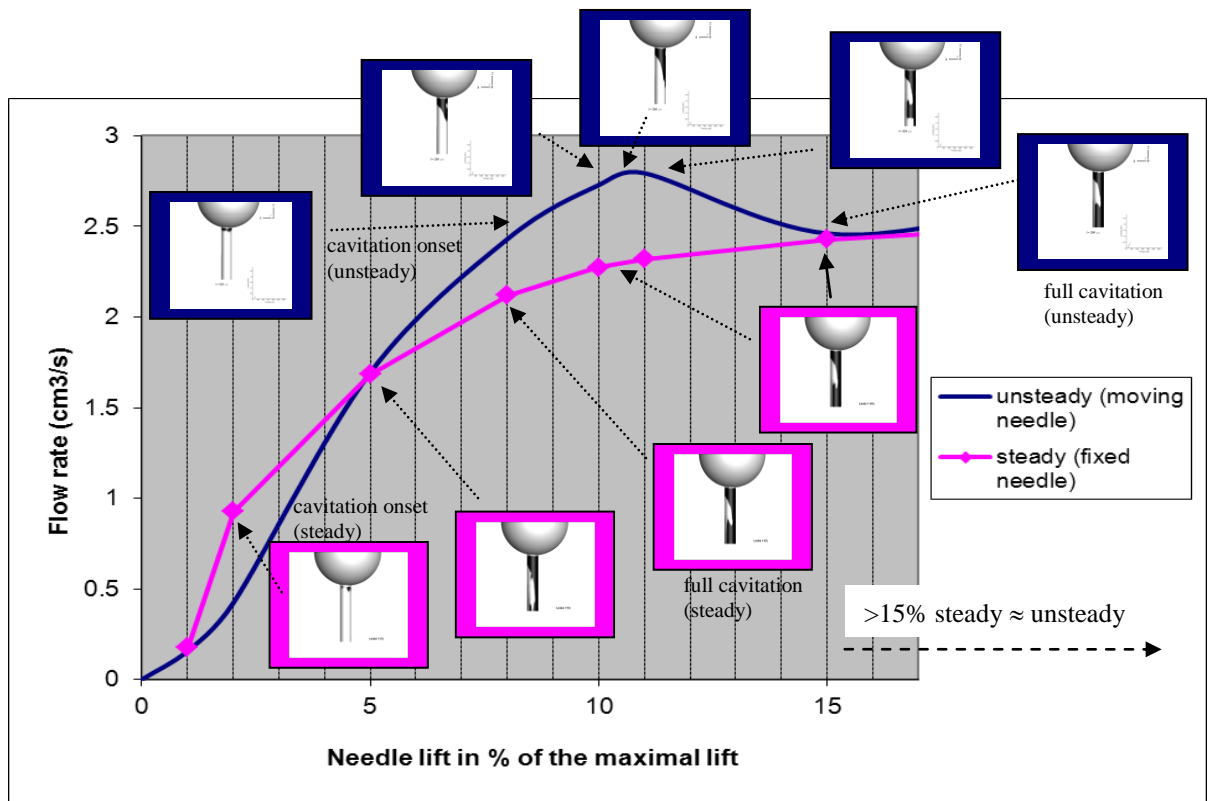


Figure 10 : comparison of the flow rate and cavitation field given by both steady and unsteady methods at low needle lift (lift < 15% of maximal lift)

## Summary and Conclusions

Cavitating flow simulations in a one-hole injector have been carried out with the EOLE CFD code. Based on comparisons with experiments the results show that the model is able to correctly represent the cavitation pattern in the hole especially the unsymmetrical extension of the vapour due to eccentricity of the hole and the variable extension of the cavitation with respect to the needle lift.

Next, comparisons have been done between both steady and unsteady needle lift models.

The steady approach remains pertinent above a certain needle lift level which is about 15% for the present injector. In this range of high lift the steady method gives very similar results as the unsteady method for the fully developed cavitation pattern and for the flow rate. Below this threshold, the steady approach becomes inaccurate as it is not able to represent the transient cavitation development at low lift and the dynamic influence of the needle motion.

This weakness of the steady method at low lift will likely be confirmed whatever the considered nozzles. However the different thresholds which have been identified here for a kind of injector and for a given operating point could be different for other injectors and injection pressures, as the level of these thresholds depend on the behaviour of the cavitation in the injector for the considered operation point.

Further simulations on other kinds of injector will be the next topic of the following studies.

## Acknowledgements

This work has been developed during a consulting study for RENAULT.

The experimental visualisation has been provided by Ecole Centrale de Lyon [7] in the framework of the NADIA\_bio program and supported by DGSIS, Région Haute Normandie and Conseil Général des Yvelines.

**References**

- [1] Habchi, Dumont and Simonin (2003): "Cavif: a 3D code for the modelling of cavitating flows in Diesel injectors", ICLASS, Sorrento, July 2003.
- [2] Xu, Bunnell and Heister (2001): "On the influence of internal flow structure on performance of plain-orifice atomizers", *Atomization and sprays*, vol. 11, pp 335-350.
- [3] Giannadakis, Papoulias, Gavaises, Arcoumanis, Soteriou and Tang: "Evaluation of the predictive capability of Diesel nozzle cavitation models", SAE 2007-01-0245
- [4] Marcer, Le Cottier, Chaves, Argueyrolles, Habchi and Barbeau (2000): "A validated numerical simulation of Diesel injector flow using a VOF method", SAE Paper 2000-01-2932.
- [5] Marcer R., Dassibat C., Argueyrolles B. : Simulation of two-phase flows in injectors with the CFD code Eole, Iclass 2008, Como Lake, 8-10 septembre 2008.
- [6] Marcer R. Audiffren C.: Simulation of unsteady cavitation on a 3D foil, V European Conference on Computational Fluid Dynamics, ECCOMAS CFD 2010, Lisbon, 14-17 June 2010.
- [7] Loïc Mées, Marc Michard. Visualisation of cavitation in a transparent diesel injector nozzle. Laboratoire de mécanique des fluides et d'acoustique (LMFA), Ecole Centrale Lyon, CNRS, Université Claude Bernard and INSA Lyon. Private communication.